

PREDICTION OF VERTICAL RESPONSE SPECTRA IN EUROPE

N. N. AMBRASEYS* AND K. A. SIMPSON†

Civil Engineering Department, Imperial College of Science Technology & Medicine, London SW7 2BU, U.K.

SUMMARY

Equations for the prediction of vertical peak and absolute acceleration spectral ordinates in terms of magnitude, source-distance and site geology are presented. Comparison to similarly derived horizontal equations shows vertical spectral values to be $1/2$ – $1/4$ of the horizontal. The influence of site geology on vertical ground motion is reduced with respect to the horizontal. Ratios of peak vertical to peak horizontal ground acceleration in the near-field of thrust faults are magnitude and distance dependent, reaching values in excess of one very near the fault of large magnitude events. For strike-slip faults the ratio exceeds one for moderate events, decreasing for larger events, and is distance independent. Spectral acceleration ratios exceed one at short periods but are less than one at intermediate and long periods, irrespective of the source mechanism.

KEY WORDS: strong-motion; attenuation; vertical response spectra; site effects; acceleration ratio; seismic design

INTRODUCTION

This is a sequel to a companion paper¹ on the attenuation of horizontal absolute acceleration spectral ordinates in Europe and adjacent areas in which we examined the prediction of horizontal response spectra in terms of source-distance, magnitude and local soil conditions.

In this paper we present equations for estimating peak vertical acceleration and vertical absolute acceleration response spectra in terms of surface-wave magnitude, source-distance, and site conditions for shallow earthquakes in the seismically active part of Europe and adjacent areas. The paper summarizes the methodology and results of the work carried out so far and updates some of our earlier conclusions which are important for the development of Eurocode 8, which does not consider vertical earthquake spectra or limits for the near-field ratio of vertical to horizontal acceleration for damaging earthquakes.

ATTENUATION OF VERTICAL PEAK ACCELERATION

In a previous paper,² using 620 records (note that this is a much reduced number from that used for horizontal peak acceleration in the same paper²) from 296 shallow European earthquakes (focal depth $h < 25$ km) in the magnitude range 4.0–7.3, the attenuation of peak vertical acceleration with distance is given by

$$\log(a_v) = -1.72 + 0.243M_s - 0.00174r - 0.750 \log(r) \quad (1)$$

with a standard deviation of 0.24 and $r^2 = d^2 + 1.9^2$. Equation (1) is shown in Figure 1.

In this study we use the same predictor variables, seismological data and procedures utilized for the derivation of the attenuation law for horizontal response spectra.¹ With these data, a two-stage regression³

* Senior Research Fellow

† Research Associate

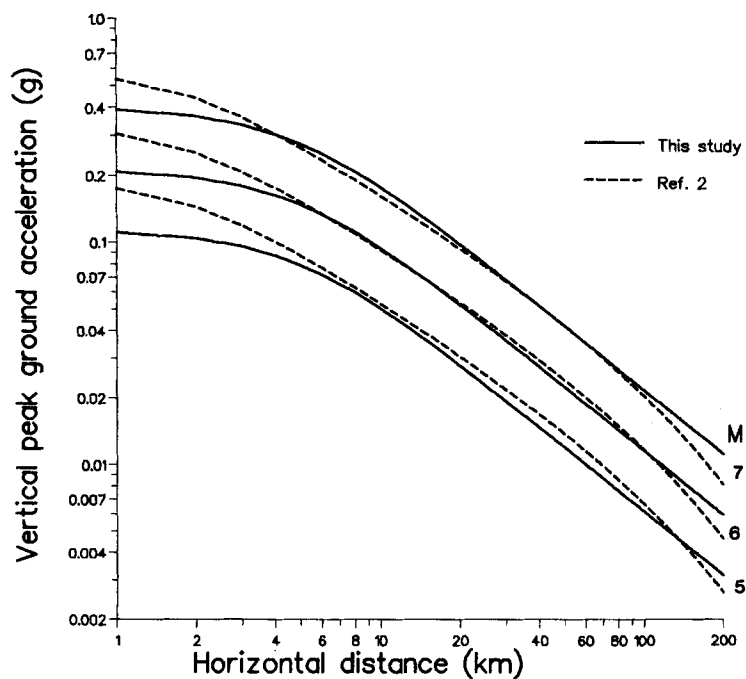


Figure 1. Comparison of values of peak vertical ground acceleration predicted for magnitudes of 5, 6 and 7 and different source-site distances by equations (1)² and (2)

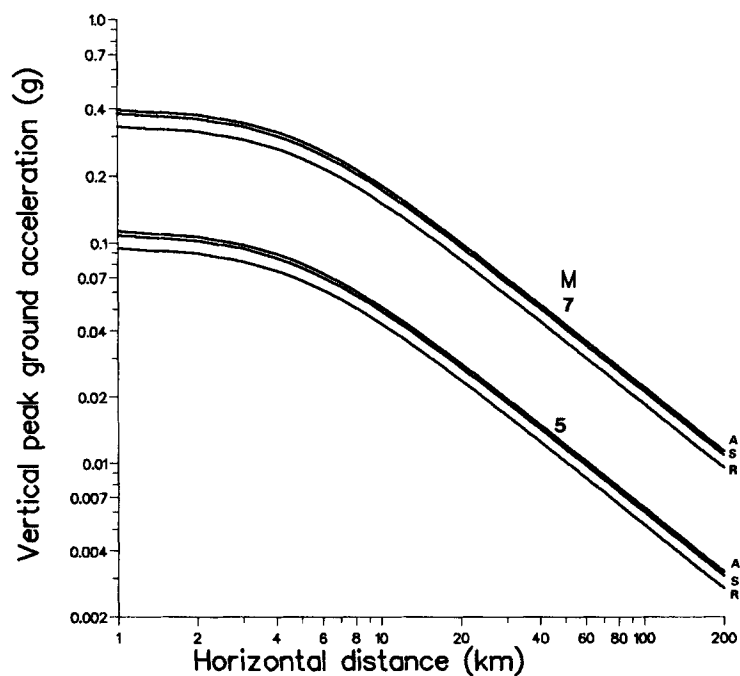


Figure 2. Predicted values of peak vertical acceleration as a function of distance for earthquake magnitudes M_s 5 and 7 and for rock (R), stiff soil (A) and soft soil (S) sites according to equation (3)

on 417 vertical records of M_s 4.0–7.9 and $h \leq 30$ km is found to be inadequate in size to determine both the anelastic and geometric distance terms, yielding an anelastic attenuation coefficient which is inadmissible. The analysis was therefore repeated setting the anelastic term to zero. The resulting equation becomes

$$\log(a_v) = -1.67 + 0.273M_s - 0.954 \log(r) \quad (2)$$

with a standard deviation of 0.27 and $r^2 = d^2 + 4.7^2$. Equation (2) is shown in Figure 1. Considering the uncertainties of the input values alone, with equations (1) and (2) having standard deviations of about 0.25, the agreement between them is about as good as can be expected.

Local soil effects are considered by subdividing sites into three categories: rock (class R with average shear wave velocity, V_s , over 30 m depth > 750 m/s), stiff soil (class A, $360 \text{ m/s} \leq V_s \leq 750 \text{ m/s}$), and soft soil (class S, $V_s < 360 \text{ m/s}$). Residuals of equation (2) for 411 records (for six records, the site type is unknown) were regressed against soil type using a dichotomous model, and the solution then added to equation (2), a procedure that gives the following results:

$$\log(a_v) = -1.74 + 0.273M_s - 0.954 \log(r) + 0.076S_A + 0.058S_S \quad (3)$$

with a standard deviation of 0.26 and $r^2 = d^2 + 4.7^2$. For rock the constants S_A and S_S are 0, for stiff soil S_A is 1 and S_S is 0, and for soft soil S_S is 1 and S_A is 0. Equation (3) for magnitudes M_s 5 and 7 and for each soil category is shown in Figure 2.

ATTENUATION OF SPECTRAL ORDINATES

To the best of our knowledge, there is only one published work on vertical spectral attenuation for the Eastern Mediterranean region.⁴ This was based on 120 triaxial records from 46 earthquakes in former Yugoslavia, Italy and Greece with two earthquake sequences in Friuli and Montenegro generating 78 per cent of the total number of records in the dataset. The study presented pseudo-velocity (PSV) response ordinates for the periods 0.02–5.0 s. In the model, the geometric attenuation term includes arbitrary constants which add to the focal distance to simulate near-field effects. Prediction of the spectral ordinates requires a specified focal depth. Site geology effects are not included.

For our study, a two-stage regression³ analysis was performed on magnitude, distance and the absolute acceleration (SA) spectral ordinates in g of the 417 records used to derive equation (2). The spectral ordinates at 5 per cent of critical damping are in the range 0.1–2.0 s at the same intervals used in the CALTECH volumes.⁵ Initial solutions again gave unacceptable anelastic coefficients so the analysis was repeated with this coefficient constrained to zero. The residuals of the 411 records with site classification from this two-stage solution were then used to derive site geology dependency in the same manner as for equation (3). The model has the overall form

$$\log(\text{SA}) = C_1 + C_2M_s + C_4 \log(r) + C_AS_A + C_SS_S + \sigma P \quad (4)$$

where $r^2 = d^2 + h_0^2$ and where P takes a value of 0 for mean values and 1 for 84-percentile values of $\log(\text{SA})$. The results are given in Table I. Figures 3–5 present vertical spectra for three different scenarios of magnitude and distance for each site class. Also shown are horizontal spectra from our earlier work.¹

DISCUSSION

We have previously¹ shown the dataset of strong-motion records used here to be representative of earthquake behaviour for the prediction of horizontal spectral ordinates in Europe based on a comparison of results for peak horizontal ground acceleration from a number of previous studies. Similarly here, we conclude that the consistency of results for peak vertical acceleration between this dataset and that derived by Ambraseys² implies the vertical spectra derived from this dataset will also be representative for Europe.

We do not present the curves of Petrovski and Marcellini⁴ since the structure of their attenuation model does not permit a valid comparison with our results. It was found that their spectra, particularly for larger events, could vary between one half and twice our spectral values for the same magnitude and distance

Table I. Coefficients of equation (4) for vertical spectral ordinates

T (s)	C_1	C_2	C_4	h_0	C_A	C_s	σ
0.10	-1.18	0.267	-1.049	5.4	0.057	0.041	0.29
0.11	-1.17	0.260	-1.033	6.0	0.078	0.066	0.28
0.12	-1.21	0.262	-1.018	6.1	0.099	0.084	0.28
0.13	-1.21	0.269	-1.038	6.6	0.103	0.081	0.28
0.14	-1.32	0.276	-1.007	6.0	0.113	0.079	0.27
0.15	-1.42	0.278	-0.959	5.2	0.117	0.092	0.27
0.16	-1.49	0.283	-0.937	4.9	0.112	0.085	0.27
0.17	-1.50	0.283	-0.920	5.3	0.110	0.084	0.28
0.18	-1.56	0.286	-0.901	5.4	0.120	0.075	0.28
0.19	-1.59	0.289	-0.901	5.6	0.125	0.064	0.27
0.20	-1.61	0.291	-0.894	5.9	0.123	0.060	0.27
0.22	-1.72	0.303	-0.868	5.5	0.099	0.062	0.27
0.24	-1.83	0.318	-0.864	5.2	0.089	0.046	0.27
0.26	-1.89	0.321	-0.850	4.7	0.083	0.023	0.27
0.28	-1.90	0.323	-0.859	5.1	0.070	0.001	0.28
0.30	-1.93	0.340	-0.906	6.2	0.064	-0.003	0.28
0.32	-2.06	0.353	-0.887	5.7	0.056	-0.004	0.28
0.34	-2.15	0.361	-0.875	5.6	0.059	0.030	0.28
0.36	-2.28	0.370	-0.839	5.0	0.062	0.046	0.27
0.38	-2.36	0.371	-0.805	4.6	0.063	0.054	0.28
0.40	-2.43	0.375	-0.791	4.2	0.067	0.068	0.28
0.42	-2.49	0.380	-0.791	3.8	0.074	0.094	0.28
0.44	-2.54	0.388	-0.804	3.9	0.074	0.101	0.28
0.46	-2.59	0.396	-0.806	4.0	0.076	0.105	0.28
0.48	-2.61	0.401	-0.821	4.6	0.073	0.104	0.28
0.50	-2.64	0.402	-0.818	4.9	0.075	0.100	0.28
0.55	-2.76	0.412	-0.800	4.9	0.074	0.095	0.28
0.60	-2.77	0.413	-0.810	6.4	0.073	0.091	0.28
0.65	-2.88	0.422	-0.786	6.1	0.058	0.089	0.29
0.70	-2.94	0.425	-0.789	5.9	0.060	0.102	0.29
0.75	-3.02	0.435	-0.802	5.7	0.071	0.111	0.30
0.80	-3.09	0.432	-0.765	5.2	0.076	0.111	0.31
0.85	-3.13	0.430	-0.750	5.0	0.078	0.125	0.31
0.90	-3.23	0.439	-0.736	4.7	0.087	0.144	0.32
0.95	-3.32	0.444	-0.714	4.5	0.085	0.141	0.32
1.00	-3.36	0.449	-0.718	4.6	0.072	0.130	0.33
1.10	-3.45	0.448	-0.684	4.5	0.062	0.128	0.32
1.20	-3.48	0.443	-0.672	4.9	0.076	0.127	0.33
1.30	-3.51	0.443	-0.680	4.7	0.073	0.120	0.33
1.40	-3.50	0.443	-0.711	5.6	0.076	0.116	0.33
1.50	-3.55	0.440	-0.697	5.3	0.082	0.123	0.34
1.60	-3.56	0.431	-0.676	5.3	0.082	0.124	0.34
1.70	-3.60	0.426	-0.654	5.1	0.078	0.113	0.35
1.80	-3.65	0.425	-0.630	5.0	0.066	0.090	0.35
1.90	-3.67	0.421	-0.612	5.5	0.057	0.091	0.35
2.00	-3.69	0.418	-0.601	5.6	0.058	0.098	0.36

scenario depending on the choice of the distance used in their model in a similar manner to that observed previously for horizontal spectra.¹

The influence of local geology is in general limited for both peak and spectral ordinates, although moderate effects are observed for stiff sites at shorter periods (<0.25 s) and soft sites at longer periods (>0.7 s). This is reduced, particularly for soft sites, when compared to the horizontal and is consistent with recent work on examining local site effects from the study of horizontal to vertical Fourier spectral ratios in which the assumption is made that the vertical component of strong-motion records is generally not amplified by surface layering.⁶⁻⁸

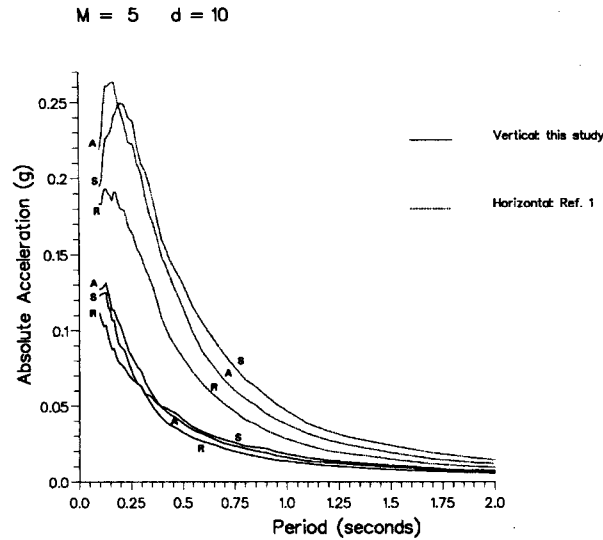


Figure 3. Vertical (this study) and horizontal¹ absolute acceleration spectra for rock (R), stiff soil (A) and soft soil (S) sites for an earthquake magnitude M_s 5 at a distance of 10 km

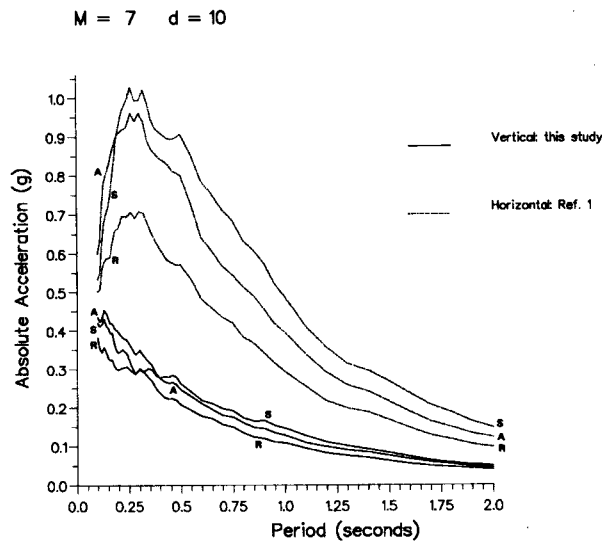


Figure 4. Vertical (this study) and horizontal¹ absolute acceleration spectra for rock (R), stiff soil (A) and soft soil (S) sites for an earthquake magnitude M_s 7 at a distance of 10 km

Figures 3–5 show that vertical spectral values are of the order of $1/2$ – $1/3$ of the corresponding horizontal spectra at short and long periods, and down to $1/4$ of the horizontal values at intermediate periods (0.5–1.0 s).

Near-field behaviour of the vertical to horizontal acceleration ratio

The question often arises of whether the peak vertical acceleration, a_v , exceeds the horizontal, a_h , and if so what are the conditions under which the acceleration ratio $q = a_v/a_h$ exceeds one. Basically, q can be derived either by combining the two attenuation equations which individually predict peak vertical and horizontal accelerations,⁹ or by performing a regression directly on the acceleration ratios.¹⁰

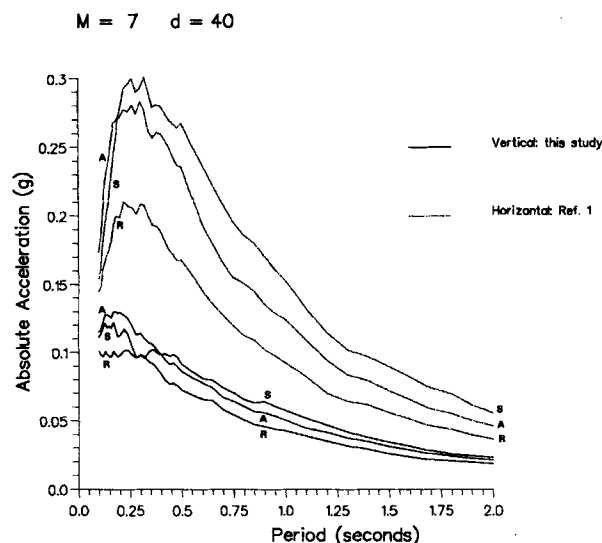


Figure 5. Vertical (this study) and horizontal¹ absolute acceleration spectra for rock (R), stiff soil (A) and soft soil (S) sites for an earthquake magnitude M_s 7 at a distance of 40 km

For the European dataset, with its rather broad magnitude and source distance content, these procedures predict that q is almost independent of M_s and distance, with a value well below one and close to 0.5. Nonetheless, it is obvious that very near the source of a shallow, normal or thrust fault-break, peak values of the vertical component of motion may exceed those of the horizontal, and that the study of the dependence of q on M_s , distance and mechanism requires a separate treatment of near-source data only. The reason for this is that the expressions for q as derived from the procedures mentioned earlier depend, to a large extent, on the magnitude bias of the sample and on the proportion of near- and far-field data in a dataset in which the amount of information from close distances for large events is usually very limited. Since for the purpose of this analysis q is only important at short distances, it would seem more appropriate not to include far-field data for its determination.

In order to investigate the behaviour of q in the near-field we examined all world-wide records available to us, generated in the near-field ($d \leq 15$ km) of shallow ($h \leq 20$ km), relatively large interplate earthquakes ($M_s \geq 6$) with peak vertical acceleration of 10 per cent g or more, which are of engineering interest. Of the 113 records identified, which belong to 34 earthquakes in the range of M_s 6.0–7.6, 59 records are associated with thrust, 46 with strike-slip and eight with normal faulting. In this global dataset, 23 records are from Europe, 88 from western U.S.A., one from New Zealand and one from Nicaragua. The distribution of this dataset in magnitude-distance space is shown in Figure 6.

We do not consider the influence of local soil conditions on q since site type is known for only 84 records and is poorly distributed with respect to the three site classes, the rock category having only eight records.

A simple regression for q on the global dataset gives

$$q = a_v/a_h = 0.855 + 0.0064M_s - 0.0057d \quad (5)$$

with a standard deviation of 0.56, showing magnitude independence and a small distance effect. Figure 7 shows the distribution of q in this global dataset and curves of q for magnitudes 5.5 and 7.5 and demonstrates that expected mean q values are close to, but do not exceed 1. This behaviour appears contrary to the observations of our dataset and the results of Abrahamson and Litehiser,⁹ Niazi and Bozorgnia¹² and Campbell,¹¹ who all show magnitude dependence, strongly so in the case of Campbell,¹¹ minor to strong distance dependence, and q values which can exceed 1.

For the European area the resulting relation is given by

$$q = a_v/a_h = -2.189 + 0.433M_s - 0.0009d \quad (6)$$

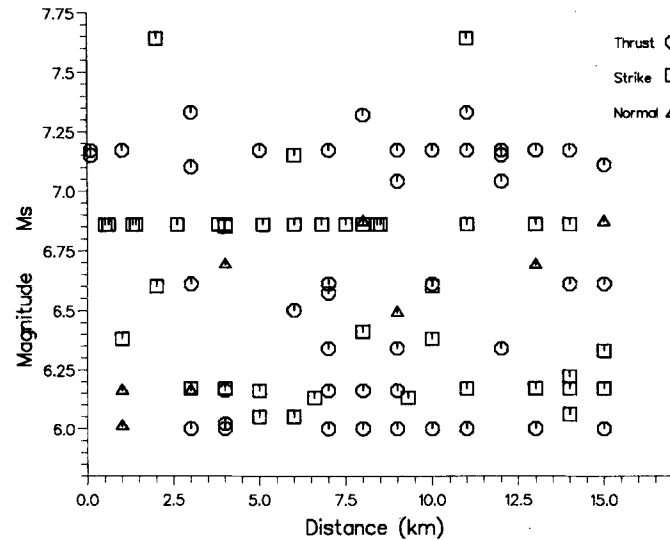


Figure 6. Distribution with respect to magnitude, distance and fault type of world-wide records available to us, generated in the near field ($d \leq 15$ km) of shallow ($h \leq 20$ km), relatively large interplate earthquakes ($M_s \geq 6$) with a peak vertical acceleration of 10 per cent g or more

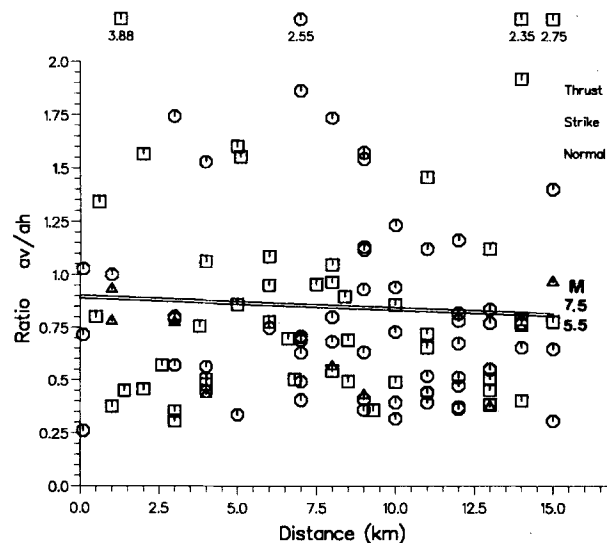


Figure 7. Distribution of the global dataset of the ratio q of peak vertical (a_v) to peak horizontal (a_h) acceleration with respect to distance and fault type, and curve of q for magnitudes M_s 5.5 and 7.5 according to equation (5). Four ratios exceed 2.0 and are shown along the top of the plot at their respective distances and with their values of q indicated

which is valid for $M_s \geq 6.0$ with a standard error of 0.36, and shows a strong dependence on M_s . However, the dataset of 23 records is considered too small to give a reliable assessment of q .

We examined the dependence of q on focal mechanism. Using the 59 records in the global dataset associated with thrust a simple regression gives

$$q = a_v/a_h = -0.132 + 0.161M_s - 0.0159d \quad (7)$$

with a standard error of 0.45.

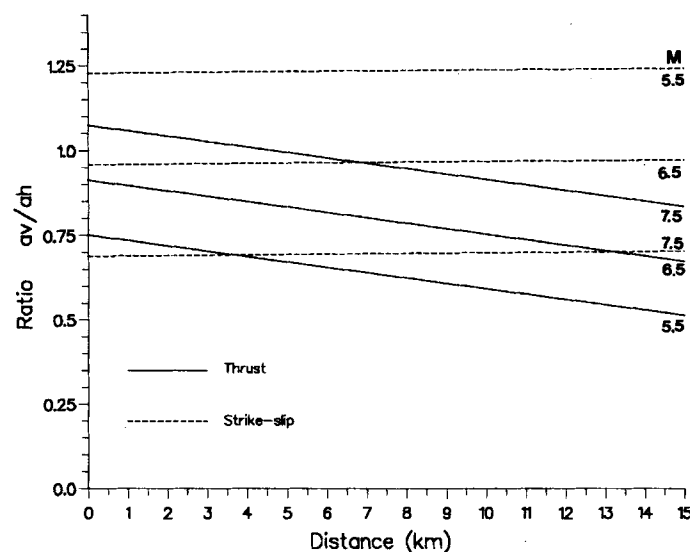


Figure 8. Curves of q with respect to distance for thrust and strike-slip faults for magnitudes M_s 5.5, 6.5 and 7.5 according to equations (7) and (8). Note the magnitude M_s 5.5 curve for strike-slip faults is the uppermost plot

For strike-slip events, the 46 records give

$$q = a_v/a_h = 2.708 - 0.269M_s + 0.0010d \quad (8)$$

with a standard error of 0.69. Both show dependence on magnitude and distance but in opposite senses. The negative coefficient of M_s in equation (8) is consistent with a stronger dependence of the horizontal (from that of the vertical) on magnitude which is compatible with strike-slip faulting, that is with increasing M_s the horizontal acceleration increases faster than the vertical. Both equations (7) and (8) give q values slightly in excess of one ($q < 1.25$), in the near-field of large thrust events and for moderate strike-slip events. Curves of q for magnitudes 5.5, 6.5 and 7.5 are shown for the thrust and strike-slip datasets in Figure 8.

It is worth pointing out that in the derivation of equations (5)–(8), the substitution of the d term by $\log(d)$, or the addition of $\log(d)$ to these equations, does not improve the fit, and that the d and $\log(d)$ coefficients no longer have anelastic or geometric meaning in the attenuation model for q .

The influence of the 'fling' or rebound of the fault as it ruptures may contribute to the observed magnitude and distance coefficients in equations (7) and (8) for thrust and strike-slip events. The fling superimposes onto wave motion a block displacement in the direction of slip proportional to magnitude (or length of rupture) and inversely proportional to distance from the fault.

Near-field behaviour of the vertical to horizontal spectral ordinate ratio

Of the 113 peak acceleration ratios identified, there are 90 for which we have full acceleration time histories from which spectral ordinate ratios can be generated. Of this set of 90, 17 are from Europe, and with records employed for the spectral ratios being those used for the generation of the individual horizontal and vertical spectra, the procedures applied to the records described elsewhere.¹ All but two of the remaining 73 records are from western U.S.A., the others are from New Zealand and Nicaragua. For these 73 records an elliptical filter¹³ with pass band 0.1–25.0 Hz was applied before determining the absolute acceleration (SA) spectral ordinates at 5 per cent of critical damping.

The attenuation model applied to the spectral ratios is as for the peak values, being linear in terms of magnitude, M_s , and distance, d , and is of the form

$$q_{SA} = SA_v/SA_h = C_1 + C_2 M_s + C_3 d + \sigma P \quad (9)$$

Table II. Coefficients of equation (9) for spectral ratios

Period T (s)	Global dataset				Thrust dataset				Strike-slip dataset			
	C_1	C_2	C_3	σ	C_1	C_2	C_3	σ	C_1	C_2	C_3	σ
0.10	1.00	0.145	-0.0334	1.25	1.48	0.081	-0.0505	1.05	1.71	0.076	-0.0412	1.56
0.11	1.26	0.127	-0.0600	1.63	1.53	0.085	-0.0760	0.96	2.54	-0.009	-0.0688	2.27
0.12	0.41	0.213	-0.0425	1.46	0.73	0.170	-0.0604	1.02	1.32	0.116	-0.0455	1.95
0.13	0.76	0.112	-0.0255	1.16	0.60	0.142	-0.0423	0.83	2.70	-0.146	-0.0311	1.54
0.14	0.92	0.074	-0.0232	1.05	1.27	0.027	-0.0385	0.69	1.84	-0.029	-0.0322	1.42
0.15	0.52	0.115	-0.0179	0.92	0.41	0.134	-0.0315	0.56	1.78	-0.051	-0.0174	1.27
0.16	0.09	0.171	-0.0197	0.79	-0.08	0.214	-0.0370	0.62	1.46	-0.031	-0.0165	1.01
0.17	-0.14	0.200	-0.0209	0.73	-0.38	0.278	-0.0504	0.71	1.46	-0.051	-0.0135	0.81
0.18	0.01	0.172	-0.0196	0.68	-0.04	0.220	-0.0481	0.67	0.91	0.022	-0.0100	0.76
0.19	-0.37	0.212	-0.0146	0.62	-0.36	0.253	-0.0417	0.62	0.57	0.057	-0.0067	0.69
0.20	-0.45	0.219	-0.0164	0.55	-0.37	0.251	-0.0438	0.56	0.61	0.043	-0.0111	0.59
0.22	-0.58	0.225	-0.0158	0.51	-0.15	0.209	-0.0418	0.53	0.14	0.099	-0.0152	0.51
0.24	-0.42	0.187	-0.0106	0.42	-0.23	0.200	-0.0304	0.49	0.38	0.049	-0.0105	0.34
0.26	-0.09	0.127	-0.0099	0.38	-0.03	0.151	-0.0245	0.43	0.57	0.009	-0.0092	0.32
0.28	0.04	0.103	-0.0097	0.37	0.11	0.116	-0.0183	0.40	0.84	-0.027	-0.0140	0.34
0.30	0.03	0.101	-0.0098	0.34	0.23	0.107	-0.0261	0.39	0.61	-0.004	-0.0096	0.28
0.32	-0.13	0.118	-0.0058	0.37	0.04	0.124	-0.0191	0.42	0.53	0.007	-0.0096	0.30
0.34	-0.44	0.169	-0.0103	0.37	-0.55	0.199	-0.0132	0.41	0.47	0.027	-0.0192	0.35
0.36	-0.03	0.104	-0.0105	0.35	-0.31	0.145	-0.0045	0.35	1.02	-0.049	-0.0234	0.37
0.38	0.21	0.065	-0.0096	0.33	-0.14	0.115	-0.0048	0.30	1.23	-0.084	-0.0196	0.40
0.40	0.25	0.048	-0.0020	0.33	-0.15	0.102	0.0049	0.28	1.34	-0.111	-0.0118	0.41
0.42	0.16	0.061	-0.0011	0.33	-0.22	0.114	0.0070	0.31	1.12	-0.082	-0.0104	0.38
0.44	0.63	-0.005	-0.0054	0.32	0.31	0.044	-0.0021	0.31	1.39	-0.124	-0.0105	0.37
0.46	1.11	-0.074	-0.0107	0.34	1.06	-0.056	-0.0135	0.34	1.46	-0.135	-0.0121	0.37
0.48	1.27	-0.097	-0.0134	0.35	1.39	-0.103	-0.0177	0.37	1.39	-0.126	-0.0140	0.37
0.50	1.15	-0.082	-0.0149	0.34	1.22	-0.084	-0.0164	0.35	1.45	-0.134	-0.0177	0.36
0.55	0.88	-0.048	-0.0101	0.31	1.00	-0.054	-0.0137	0.32	1.38	-0.128	-0.0163	0.31
0.60	1.45	-0.127	-0.0146	0.37	1.51	-0.125	-0.0174	0.35	1.91	-0.198	-0.0191	0.41
0.65	1.49	-0.129	-0.0159	0.39	1.39	-0.098	-0.0212	0.40	2.10	-0.231	-0.0176	0.40
0.70	1.53	-0.142	-0.0109	0.45	1.59	-0.134	-0.0153	0.50	2.01	-0.219	-0.0168	0.42
0.75	1.42	-0.131	-0.0064	0.44	1.48	-0.125	-0.0110	0.51	1.66	-0.174	-0.0091	0.39
0.80	1.61	-0.162	-0.0056	0.38	1.42	-0.122	-0.0107	0.44	1.93	-0.222	-0.0021	0.35
0.85	1.57	-0.152	-0.0102	0.31	1.17	-0.082	-0.0156	0.34	2.15	-0.252	-0.0046	0.30
0.90	1.48	-0.132	-0.0123	0.29	1.13	-0.076	-0.0127	0.28	2.02	-0.224	-0.0123	0.31
0.95	1.46	-0.127	-0.0119	0.28	1.16	-0.075	-0.0130	0.27	1.97	-0.212	-0.0128	0.31
1.00	1.47	-0.128	-0.0100	0.28	1.09	-0.067	-0.0115	0.26	2.13	-0.236	-0.0124	0.31
1.10	1.37	-0.109	-0.0114	0.34	0.60	-0.006	-0.0023	0.32	2.39	-0.265	-0.0185	0.35
1.20	1.33	-1.101	-0.0117	0.38	0.21	0.047	0.0019	0.32	2.94	-0.339	-0.0217	0.43
1.30	1.34	-0.102	-0.0082	0.42	-0.25	0.096	0.0187	0.32	3.36	-0.396	-0.0230	0.48
1.40	1.18	-0.072	-0.0108	0.39	-0.31	0.108	0.0151	0.27	2.89	-0.323	-0.0240	0.44
1.50	1.13	-0.069	-0.0104	0.33	-0.13	0.080	0.0126	0.23	2.54	-0.272	-0.0207	0.37
1.60	1.07	-0.060	-0.0087	0.36	-0.26	0.097	0.0153	0.22	2.38	-0.251	-0.0188	0.36
1.70	1.17	-0.075	-0.0077	0.37	-0.21	0.093	0.0147	0.25	2.54	-0.277	-0.0165	0.35
1.80	1.00	-0.055	-0.0043	0.34	-0.24	0.097	0.0179	0.30	2.37	-0.257	-0.0139	0.31
1.90	1.12	-0.072	-0.0053	0.33	-0.14	0.092	0.0125	0.33	2.72	-0.312	-0.0130	0.28
2.00	1.26	-0.093	-0.0063	0.31	0.05	0.075	0.0038	0.32	2.94	-0.350	-0.0098	0.26

where σ is the standard deviation of q_{SA} and P takes a value of 0 for mean values and 1 for 84-percentile values of q_{SA} . Results for the full dataset and separate treatments of the thrust and strike-slip datasets are presented in Table II. Plots of spectral ratios for magnitudes 5.5 and 7.5 at fault a distance of 5 km and a magnitude 7.5 at 15 km are shown in Figures 9–11. Results from the European dataset show large fluctuations in the magnitude and distance coefficients from significant positive to significant negative values over one period step and are not considered reliable.

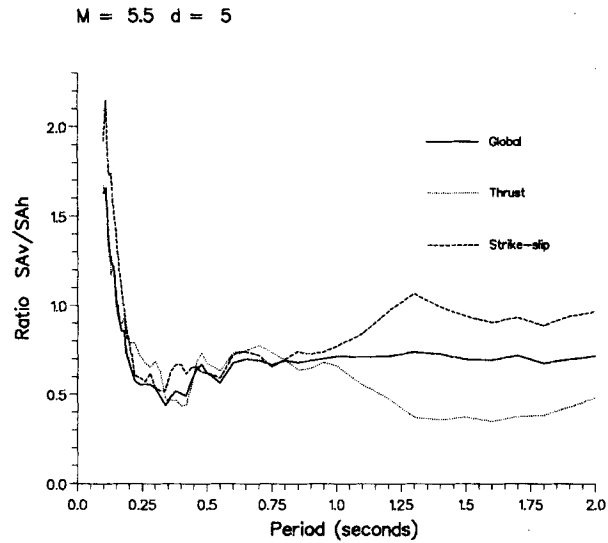


Figure 9. Spectral acceleration ratios, $q_{SA} = SA_v/SA_h$, for global dataset and for thrust and strike-slip faults for an earthquake magnitude M_S 5.5 at a distance of 5 km

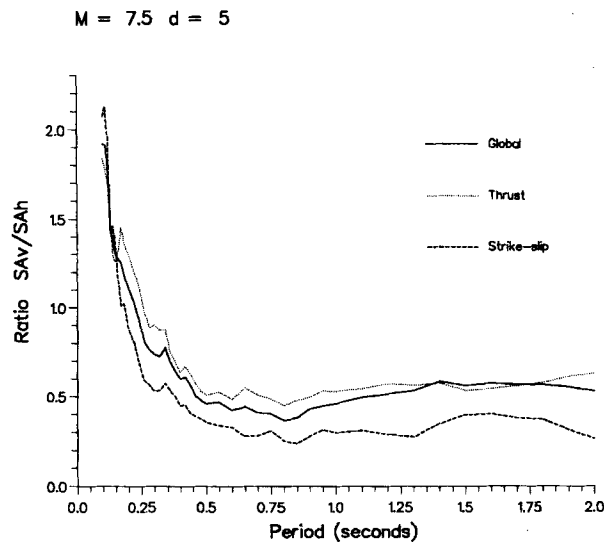


Figure 10. Spectral acceleration ratios, $q_{SA} = SA_v/SA_h$, for global dataset and for thrust and strike-slip faults for an earthquake magnitude M_S 7.5 at a distance of 5 km

Coefficients for thrust and strike-slip also fluctuate between positive and negative values, although generally over wider period ranges, except where values are close to zero. It is interesting to note that the largest coefficients occur at short periods for thrust data but at long periods for the strike-slip data. This may be linked to the 'fling' factor described previously which would be expected to only influence a limited period band. Spectral ratios are seen to greatly exceed one at short periods, independent of the fault mechanism. For longer periods, however, the ratio for the two different mechanisms can vary significantly, from one to nearly zero, dependent on magnitude and distance.

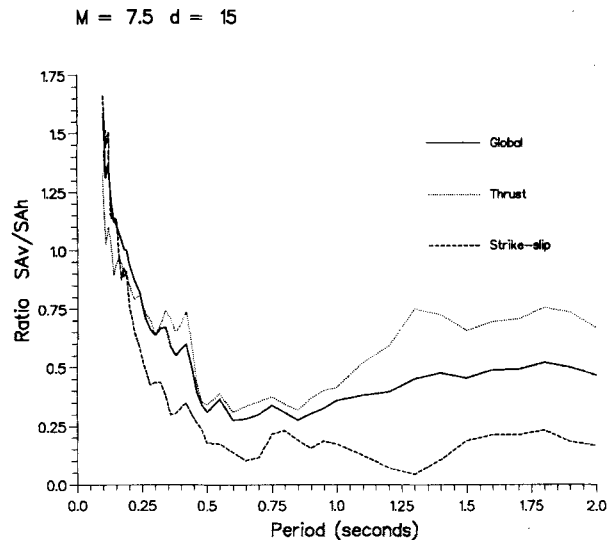


Figure 11. Spectral acceleration ratios, $q_{SA} = SA_v/SA_h$, for global dataset and for thrust and strike-slip faults for an earthquake magnitude $M_s 7.5$ at a distance of 15 km

CONCLUSIONS

We find that for the European dataset, vertical spectra vary between 1/2 and 1/4 of their corresponding horizontal values. However, these are average values over distances of 100 km or more and they should differ from near-source conditions.

We find that the spectral shape and periods at which the maximum values occur are different for vertical and horizontal motions, and that on average vertical spectral values decay more slowly with period. These differences are large enough to warrant consideration in the definition of design spectra for Eurocode 8.

Local foundation conditions do not significantly influence vertical spectra. However, we find that for short periods both horizontal and vertical spectra for soft sites (S) show systematically smaller amplification than for stiff sites (A). This trend is reversed at intermediate and long periods. If this trend is genuine it may suggest de-amplification of the high frequency motion in thin superficial soft soil deposits due to high straining.

Very near the source of large thrust earthquakes the average value of the acceleration ratio q may exceed one but falls off with distance. For strike-slip faults the available data suggest that q reaches one only for moderate size events, decreasing for larger events, and that distance variations in the near-field have little effect on its value. The European dataset suggests that q overall remains close to the commonly accepted 2/3 value proposed by Newmark and Hall.¹⁴ Spectral acceleration ratios q_{SA} exceed one at short periods but are typically less than one for intermediate and long periods.

ACKNOWLEDGEMENTS

The authors would like to thank J. J. Bommer, S. K. Sarma, M. Free and M. Srbulov for assistance in the preparation of data and for useful ideas and suggestions. The contributions of R. Berardi, B. Mohammadioun and D. Rinaldis are also gratefully acknowledged, as is the co-operation of all those individuals and agencies who contributed data. This work is supported by the European Council Environment Research Programme, contract EV5V-CT94-0490 Climatology and Natural Hazards, DG XII, Bruxelles.

REFERENCES

1. N. N. Ambraseys, K. A. Simpson and J. J. Bommer, 'Prediction of horizontal response spectra in Europe', *Earthquake eng. struct. dyn.* **25**, 371–400 (1996).

2. N. N. Ambraseys, 'The prediction of earthquake peak ground acceleration in Europe', *Earthquake eng. struct. dyn.* **24**, 467–490 (1995).
3. S. K. Sarma, 'Fortran program ATTEN', *ESEE Internal Report*, Imperial College of Science, Technology and Medicine, London, 1994.
4. D. Petrovski and A. Marcellini, 'Prediction of seismic movement of a site—statistical approach', *Proc. U.N. seminar on predict. of earthquake*, Paper SC. Tech./Sem. 16/R. 16, Lisbon, 14–18 November 1988.
5. CIT, 'Analyses of strong motion earthquake accelerograms—response spectra. Vol. III, Part A', *Report No. EERL 72-70*, Earthquake Engineering Research Laboratory, California Institute of Technology, Pasadena, 1972.
6. N. P. Theodulidis and P.-Y. Bard, 'Horizontal to vertical spectral ratio and geological conditions: an analysis of strong motion data from Greece and Taiwan (SMART-1)', *Soil dyn. earthquake eng.* **14**, 177–197 (1995).
7. K. Atakan and J. Havskov, 'Local site effects in northern North Sea based on single-station spectral ratios of OBS recordings', *Terra nova* (in press).
8. Y. Nakamura, 'A method for dynamic characteristics estimation of subsurface using microtremor on the ground surface', *Quart. report railway tech. res. inst.* **30**(1), 25–33 (1989)—not seen.
9. N. A. Abrahamson and J. J. Litehiser, 'Attenuation of vertical peak acceleration', *Bull. seism. soc. Am.* **79**, 549–580 (1989).
10. N. N. Ambraseys and J. J. Bommer, 'The attenuation of ground accelerations in Europe', *Earthquake eng. struct. dyn.* **20**, 1179–1202 (1991).
11. K. W. Campbell, 'A study of the near-source behaviour of peak vertical acceleration', *EOS* **63**, 1037 (1982).
12. M. Niazi and Y. Bozorginia, 'Behaviour of near-source peak horizontal and vertical ground motions over SMART-1 array, Taiwan', *Bull. seism. soc. Am.* **81**, 715–732 (1991).
13. J. M. H. Menu, 'Engineering study of near-field earthquake strong-motions', *Ph. D. Thesis*, University of London, 1986.
14. N. M. Newmark and W. J. Hall, 'Earthquake spectra and design', Earthquake Engineering Research Institute, Berkeley, 1982.